



OPEN In vitro characterization of radiofrequency ablation lesions in equine and swine myocardial tissue

Eva Buschmann¹✉, Glenn Van Steenkiste¹, Mattias Duytschaever², Patrick Segers³, Lara Ibrahim⁴, Gunther van Loon¹ & Annelies Decloedt¹

Radiofrequency ablation is a promising technique for arrhythmia treatment in horses. Due to the thicker myocardial wall and higher blood flow in horses, it is unknown if conventional radiofrequency settings used in human medicine can be extrapolated to horses. The study aim is to describe the effect of ablation settings on lesion dimensions in equine myocardium. To study species dependent effects, results were compared to swine myocardium. Right ventricular and right and left atrial equine myocardium and right ventricular swine myocardium were suspended in a bath with circulating isotonic saline at 37 °C. The ablation catheter delivered radiofrequency energy at different-power-duration combinations with a contact force of 20 g. Lesion depth and width were measured and lesion volume was calculated. Higher power or longer duration of radiofrequency energy delivery increased lesion size significantly in the equine atrial myocardium and in equine and swine ventricular myocardium ($P < 0.001$). Mean lesion depth in equine atrial myocardium ranged from 2.9 to 5.5 mm with a diameter ranging from 6.9 to 10.1 mm. Lesion diameter was significantly larger in equine tissue compared to swine tissue ($P = 0.020$). Obtained data in combination with estimated wall thickness can improve lesion transmural which might reduce arrhythmia recurrence. Optimal ablation settings may differ between species.

Abbreviation

RF: radiofrequency.

Introduction

Radiofrequency (RF) catheter ablation has been described as a successful treatment for atrial tachycardia and an accessory pathway in horses^{1,2}. This technique is based on application of RF energy to the myocardium. Flow of the RF current through the myocardium results in resistive tissue heating. The heat then conducts passively into the deeper layers of the myocardium. Tissue exposed to 50 °C or more will show irreversible coagulation necrosis and evolve into nonconducting scar³. By destroying the arrhythmogenic tissue and thereby treating the underlying cause of the arrhythmia, this technique can resolve the arrhythmia and reduce the recurrence rate. In human medicine, recurrence of arrhythmia is shown to be due to non-transmural scars or gaps at the site of ablation⁴. Durable lesions should be continuous and transmural, thereby inducing permanent loss of conduction while avoiding complications and collateral damage⁴. Key determinants of ablation lesion size are, amongst others, duration of energy application and applied power⁵. Power and duration can be increased to increase lesion depth and ablation efficacy. However, excessive energy delivery can cause complications such as cardiac perforation and collateral damage to intracardiac and extracardiac structures⁶. Therefore, a careful balance should be obtained between applying sufficient energy to reach lesion transmural but not too much energy to avoid complications. The magnitude of current delivered to the tissue is inversely related to the impedance between the ablation catheter and the indifferent electrode. Creation of a RF lesion results in a drop in impedance. The magnitude of this drop correlates with lesion size and can therefore be used as real-time marker of lesion formation³.

In current practice, similar settings are used in horses and in human patients. Horses, however, have a thicker myocardial wall and a higher blood flow, which might have an effect on the final lesion size during RF ablation.

¹Department of Internal Medicine, Reproduction and Population Medicine, Faculty of Veterinary Medicine, Equine Cardioteam Ghent University, Ghent University, Merelbeke, Belgium. ²Department of Cardiology, AZ Sint-Jan, Bruges, Belgium. ³Institute of Biomedical Engineering and Technology, Faculty of Engineering and Architecture, Ghent University, Ghent, Belgium. ⁴Department of Morphology, Imaging, Orthopedics, Rehabilitation and Nutrition, Ghent University, Merelbeke, Belgium. ✉email: eva.buschmann@ugent.be

Furthermore, different animal species, such as swine, dogs or cows, are commonly used in ex vivo and in vivo ablation studies for human medicine, without taking into account the possible differences between species.

The first objective of this study was to describe the effect of ablation settings on lesion dimensions in equine myocardial tissue. This information is needed to safely create transmural lesions in equine patients to minimize arrhythmia recurrence after RF ablation. The second objective was to compare lesion dimensions induced in equine and swine myocardium to evaluate potential species and tissue related differences.

Materials and methods

Animals

No live animals were used in this study. Equine hearts were harvested from horses euthanized for non-cardiovascular reasons at the Faculty of Veterinary Medicine, Ghent University ($n=5$), or collected from the slaughterhouse ($n=5$). These hearts were collected from 10 warmblood horses, 5 geldings and 5 mares, with a median age of 16 [4–29] years. The median height and weight of the horses euthanized at the faculty are 166 [160–170] cm and 500 [493–600] kg. Auscultation revealed no abnormalities. No information about height, weight and auscultation of the horses from the slaughterhouse was available. Eleven swine hearts were collected from the slaughterhouse. Pigs had an age of 6–8 months and a weight of ± 120 kg. To minimize variation in wall thickness, tissue strips were collected from the same location in each heart. In each equine and swine heart, smooth-surfaced myocardial strips of the right ventricular free wall were harvested. These strips were bordered cranially by the subatrial papillary muscle, dorsally by the parietal cusp of the tricuspid valve, caudally and ventrally by the attachment of the interventricular septum. In each equine heart, similar smooth-surfaced myocardial strips from the right and left atrial free wall were collected. In each equine heart, two right ventricular strips, one right atrial and one left atrial strip were collected and, in each swine heart, one right ventricular strip was obtained. A mold of 5 cm x 13 cm was used to standardize the size of the myocardial strips. Myocardial strips were stored in isotonic saline at room temperature until the start of the experiments. In vitro ablation was started within 30 to 60 min after euthanasia or slaughter.

In vitro set-up

An in vitro model was assembled to mimic physiological conditions of the equine heart during ablation (Fig. 1). RF energy was delivered on smooth-surfaced tissue from the right ventricle and right and left atrium of the equine hearts and on the right ventricle of the pig hearts. The strips of myocardial tissue were suspended in a heated water bath with isotonic saline at 37 °C. Blood flow was imitated by a peristaltic perfusion pump circulating the saline in the bath. Pump settings were such that a flow velocity of 0.35 m/s across the endocardial surface was realized, based on the flow in the vena cava caudalis of horses measured by pulsed-wave Doppler

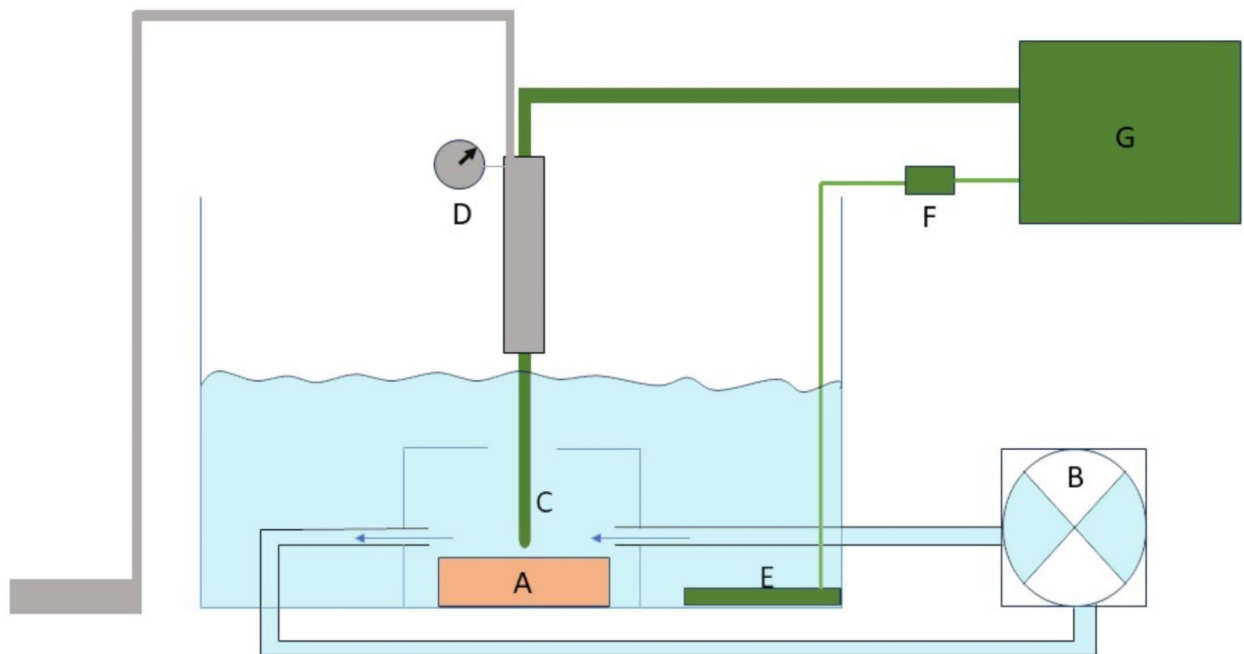


Fig. 1. Schematic representation of the in vitro set-up. Myocardial tissue (A) was suspended in a bath with isotonic saline at 37 °C. Flow was created by a pump (B) with flow velocity at the level of the myocardial tissue set at 0.35 m/s. The ablation catheter (C) was mounted in a holder with a dynamometer (D) to maintain the catheter tip perpendicular to the tissue with a constant contact force of 20 g. The indifferent electrode (E) was placed in the bath and a resistor of 25 Ω (F) was placed between the indifferent electrode and the ablation generator (G).

with transthoracic ultrasound. A 7.5 F irrigated ablation catheter (Intellanav OI, Boston Scientific, Machelen, Belgium) was mounted in a holder with a dynamometer to maintain the catheter tip perpendicular to the tissue with a constant contact force of 20 g. The indifferent electrode was placed in the bath, with an additional power resistor of 25 Ohm between the indifferent electrode and the generator to mimic the physiologic impedance of 120 Ohm in horses (unpublished data), as well as in humans⁷.

Ablation protocol

The ablation catheter was connected to the RF generator (Stockert GmbH 70 ST-1004 RF, Johnson & Johnson, Brussel, Belgium). Different combinations of RF power and duration were tested while recording the current, catheter tip temperature and circuit impedance. Impedance drop was measured as the difference between baseline impedance at the start of RF application and impedance at the end of RF delivery. Radiofrequency energy was delivered in power-controlled mode. During energy delivery, the ablation catheter was irrigated with saline at room temperature at a rate of 30 ml/min. For right ventricular tissue, seven combinations were tested and repeated three times on each equine heart and two times on each swine heart: 30 W 30 s; 30 W 60 s; 40 W 30 s; 40 W 60 s; 50 W 30 s; 50 W 60 s and 60 W 10 s. On one swine heart, the combinations could only be tested once. On atrial tissue, four combinations of power and duration were tested: 40 W 30 s; 40 W 60 s; 50 W 30 s and 60 W 10 s. For each heart, these combinations were repeated three times on right atrial tissue and two times on left atrial tissue. The different settings were applied at random.

After ablation, the lesions were excised and transverse sections were made along the maximum diameter of the lesions. The transverse sections were incubated with 2,3,5-triphenyl tetrazolium chloride for 10 min. The reaction was stopped with 10% formalin after staining. The viable myocardium becomes dark red after staining whereas the necrotic ablation lesion remains unstained. Photographs were obtained of the tissue sections along with a calliper. Maximum depth (A), maximum diameter (B), depth at maximum diameter (C) and lesion surface diameter (D) were measured on the photographs by a blinded observer using ImageJ (Fig. 2). These measurements were used to calculate the lesion volume by using the equation for an oblate ellipsoid⁶:

$$\text{Lesion volume} = \left[0.75\pi \left(\frac{B}{2} \right)^2 (A - C) \right] - \left[0.25\pi \left(\frac{D}{2} \right)^2 (A - 2C) \right]$$

Statistical analysis

Normality of continuous data was assessed by inspection of histograms and Q-Q plots. Normally distributed data are presented as mean \pm standard deviation and non-normally distributed data as median [range]. First, one-way ANOVA was used to compare the effect of power-duration combination on maximum lesion depth, maximum diameter and volume for the right ventricle, right atrium and left atrium separately. Post hoc tests

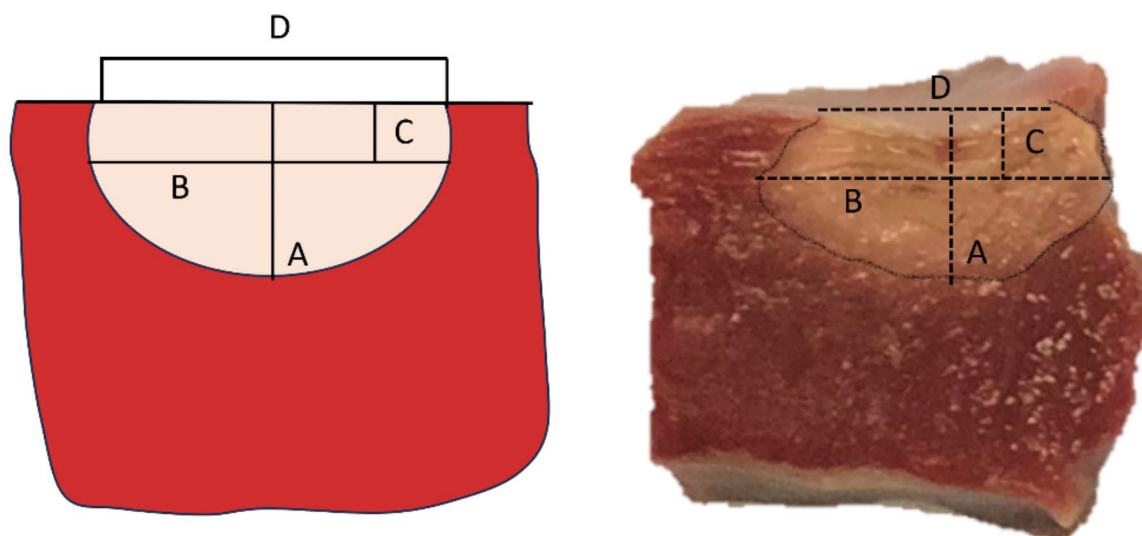


Fig. 2. Measurements to analyse lesion dimensions and calculate the volume are shown on a schematic representation (left) and on a tissue sample of an ablation lesion in equine ventricular myocardium (right). The maximum depth (A), maximum diameter (B), depth at maximum diameter (C) and surface diameter (D) were measured.

were performed with Bonferroni corrections for multiple comparisons. Then, multiple linear regression was used to test if power and duration predicted lesion size in the right ventricle. The 60 W 10 s setting was excluded from the model because its short duration resulted in smaller lesion sizes compared to lower power settings with longer durations. A general linear model was used to test the effect of tissue type (right ventricle, right atrium and left atrium) on lesion depth, diameter, volume and wall thickness in the equine myocardium, with setting included as an independent factor. Similarly, a general linear model was created to compare lesion depth, diameter and volume between horses and pigs. Pearson's correlation coefficient was used to assess correlation between wall thickness and lesion depth for lesions in the right atrium. Spearman's correlation coefficient was used to assess correlation between impedance drop and lesion dimensions. Subsequently, a Mann-Whitney U Test was used to compare impedance drop, average and maximum impedance between species. Categorical variables are presented as percentages and were compared by Pearson's chi-square test. A *p* value of <0.05 was considered significant. Statistical analyses were performed by using SPSS (SPSS Statistics 25, IBM, Brussels, Belgium).

Results

A total of 398 ablation lesions were analysed in the equine heart, of which 202 lesions were in the right ventricle, 118 in the right atrium and 78 in the left atrium. A total of 135 ablation lesions were analysed in the pig heart. Radiofrequency applications that did not induce a visible lesion were excluded. Figure 3 and table S1 (table is available in Supplemental Material on-line) shows ablation lesion dimensions for different power-duration combinations in the right ventricle, right atrium and left atrium of 10 equine hearts and the right ventricle of 11 pig hearts. There were no steam pops for any setting, tissue type or species.

Equine right ventricle

Typical ablation lesions for each setting are displayed in Fig. 4. The median right ventricular wall thickness was 16.7 [5.3–26.7] mm. Mean lesion depth ranged from 3.3 to 5.8 mm with a diameter ranging from 7.7 to 10.8 mm. One-way ANOVA showed a significant difference in lesion depth, diameter and volume for the different ablation settings ($P < 0.001$ for depth, diameter and volume), with higher power or longer duration of RF energy delivery resulting in increased lesion dimensions. Maximal lesion volume and lesion depth were obtained with a power-duration combination of 40 W 60 s and 50 W 60 s (244 ± 116 and 239 ± 114 mm³; 5.8 ± 1.1 and 5.7 ± 1.2 mm, respectively). This was significantly larger compared to lesion sizes induced by all other settings ($P < 0.001$). No significant differences of lesion size were found between application of 40 W 60 s and 50 W 60 s. High power short duration (60 W 10 s) showed the smallest lesion dimensions, with a lesion depth significantly smaller compared to all other settings ($P < 0.001$) except for 30 W 30 s.

The lesion size data were fitted to a regression model. Power and duration were correlated with lesion depth, width and volume ($P < 0.001$ for each parameter). An increase of 10 W led to an increase of 0.5 mm, 1 mm and 4.4 mm³ in lesion depth, diameter and volume, respectively. Lesion depth, diameter and volume increased with 0.4 mm, 0.5 mm and 2.9 mm³ respectively, for an increase in ablation duration of 10 s.

Equine right and left atrium

The median right and left atrial wall thickness was 4.7 [1.4–13.4] mm and 9.4 [5.0–21.3] mm, respectively. Mean lesion depth and diameter were between 2.9 and 4.8 mm and 7.2–10.1 mm, respectively for the right atrium and 3.2–5.2 mm and 6.9–10.1 mm for the left atrium. The same trends as in the right ventricle were observed: both increasing RF power or duration increased lesion dimensions. One-way ANOVA showed a significant ($P < 0.001$) difference in lesion depth, diameter and volume between the different ablation settings. The 60 W 10 s application produced the smallest lesions with a significantly smaller lesion depth ($P < 0.05$ for the right atrium and $P < 0.01$ for the left atrium). In the right atrium, lesion depth was significantly higher using 40 W 60 s (4.8 ± 1.6 mm) compared to 40 W 30 s (3.8 ± 1.1 mm, $P = 0.019$) and 60 W 10 s (2.9 ± 1 mm, $P < 0.001$). In the left atrium, lesion depth did not differ significantly between 40 W 30 s, 40 W 60 s and 50 W 30 s, although there was a trend for deeper lesions using 40 W 60 s.

Due to the thin wall of the right atrium, increasing the power and duration led to transmural lesions. In the right atrium, 63 of 118 lesions were transmural (53%). The setting had a significant effect on lesion transmural ($P < 0.001$). A power and duration of 40 W 30 s, 40 W 60 s and 50 W 30 s induced 66%, 70% and 60% transmural lesions, respectively, while only 17% of the lesions were transmural with 60 W 10 s. Lesion depth was limited by wall thickness and a positive correlation was found ($P < 0.001$, $r = 0.585$) between lesion depth and wall thickness. In the left atrium, only 4 out of 78 lesions were transmural, with no significant correlation between depth and wall thickness. Three of the transmural lesions were induced by 40 W 60 s and one lesion by 50 W 30 s.

Tissue differences

Significant differences in lesion depth and volume were noticed between the atrial and ventricular strips ($P < 0.001$). Depth of the lesions in the right atrium was significantly smaller than those in the left atrium ($P = 0.007$) and right ventricle ($P < 0.001$). The right atrial wall was significantly thinner than the left atrial wall and right ventricular wall ($P < 0.001$).

Pig hearts

Typical ablation lesions for each setting in right ventricular swine tissue are presented in Fig. 4. The median right ventricular wall thickness was 7.8 [4.1–14.3] mm. Mean lesion depth and diameter were between 2.8 and 5.9 mm, and 6.3 and 10.4 mm, respectively. Lesion dimensions followed a similar trend as in the horse: an increase in power or duration increased the lesion depth, diameter and volume. Lesion diameter was significantly larger in

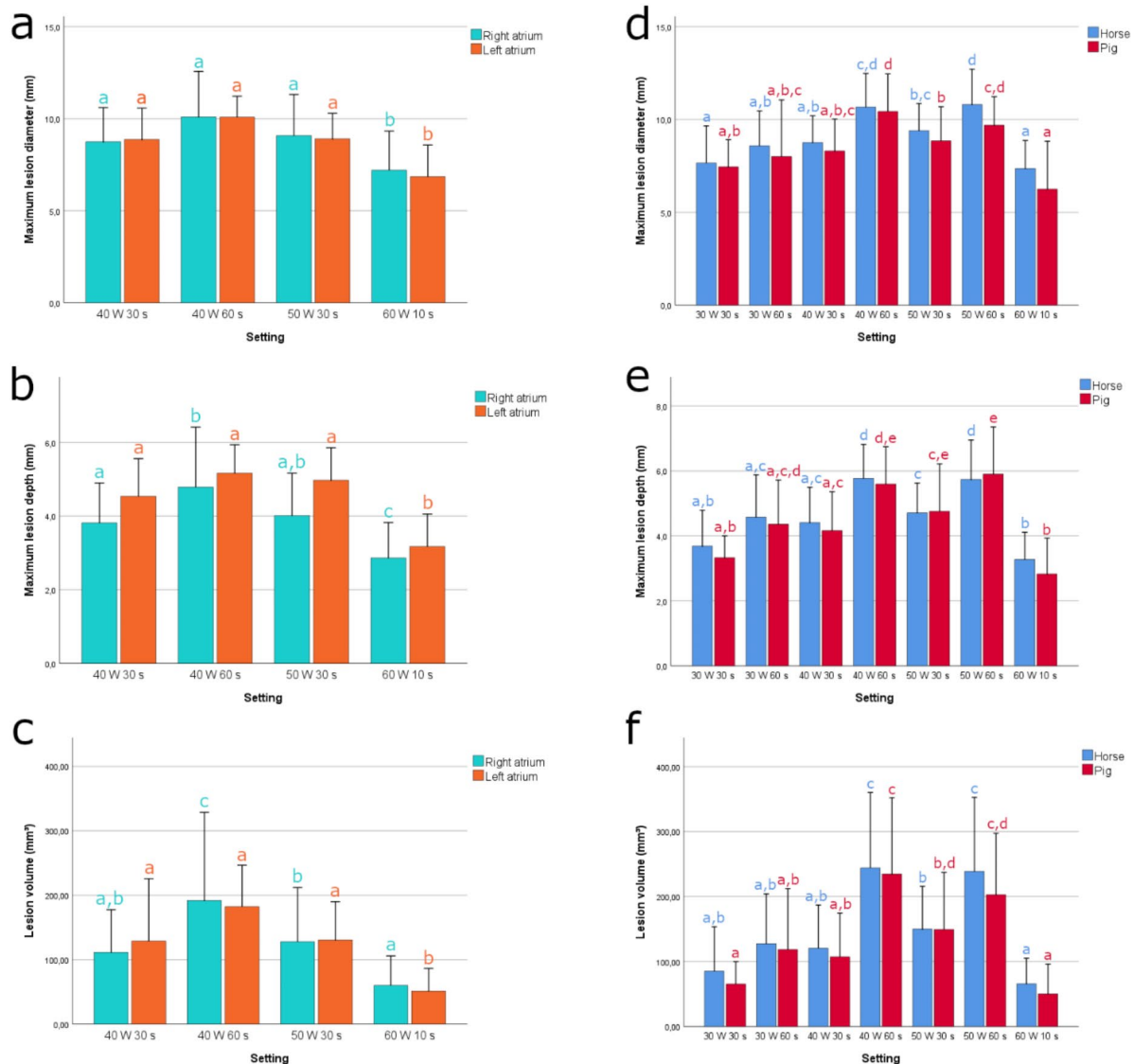


Fig. 3. Bar charts present the maximum lesion diameter (a, d), lesion depth (b, e) and lesion volume (c, f) for each setting. Chart a–c present lesion dimensions for the equine right and left atrium. Chart d–f present lesion dimensions for equine and swine right ventricle. Error bars indicate the standard deviation. Bars with different letters indicate significant differences between settings ($P < 0.05$) within each group (right atrium, left atrium and equine right ventricle and swine right ventricle).

equine tissue compared to swine tissue ($P = 0.020$) but no significant difference could be observed between both tissues for lesion depth and volume.

Impedance drop

Impedance drops and average impedance for each setting and each tissue type are presented in Table S1. Impedance drop for the lesions induced in equine and swine tissue was positively correlated with lesion depth, diameter and volume ($P < 0.001$ and $r = 0.4$ for each parameter). Impedance drop in swine ventricular tissue was significantly larger than in equine ventricular tissue ($P < 0.001$). Maximum and average impedance were also significantly larger in swine ventricular tissue ($P < 0.001$).

Discussion

The major findings of this in vitro study are as follows: (1) An increase in ablation power and/or duration leads to an increase in lesion depth, diameter and volume. (2) Impedance drop is correlated with lesion depth, diameter and volume. (3) Lesion diameter was significantly larger in equine compared to swine ventricular tissue.

Applying RF energy at a higher power or longer duration increased the lesion size in the ventricle, as well as in the right and left atrium. Higher power has been described to result in larger current density at the ablation electrode and can therefore increase the amount of tissue heating, resulting in larger lesion size^{3,8–10}. Likewise,

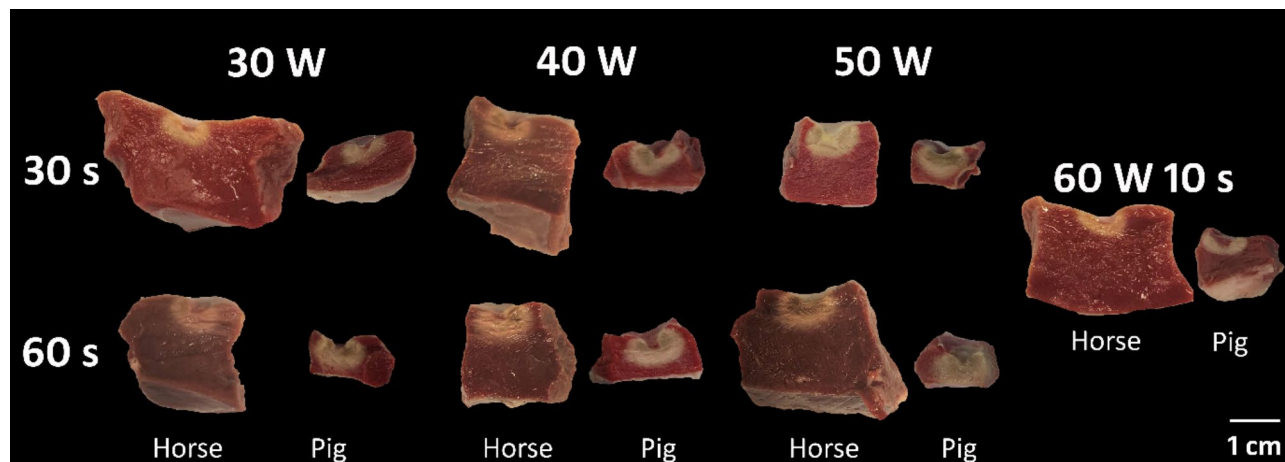


Fig. 4. Ablation lesions in the right ventricular wall of equine and swine hearts after 2,3,5-triphenyl tetrazolium chloride staining. Viable myocardium is stained dark red, whereas the necrotic ablation lesion remains unstained. It is noted that an increase in power or duration of radiofrequency energy led to an increase in lesion depth, diameter and volume.

lesion size increases monoexponentially with longer duration¹¹. In addition to power and duration, catheter-tissue contact is a crucial determinant of lesion size. In this *in vitro* set-up, a constant contact force of 20 g was used which is based on the recommended contact force in human medicine¹². In an *in vivo* situation, catheter-tissue contact is variable due to cardiac and respiratory motion and catheter orientation, which results in smaller lesions than ablation with similar power and constant contact¹³. To take into account these key factors of lesion formation, the ablation index has been developed. This is a lesion quality marker incorporating contact force, power and duration into a weighted formula and is correlated with lesion dimensions¹⁴. The target ablation index should be adapted to the wall thickness to induce transmural lesions. An ablation index of 450–500 was successfully used to isolate the caudal vena cava and pulmonary veins in horses¹⁵.

In human medicine, recurrence of arrhythmia after RF ablation is mostly due to non-transmural lesions⁴. This is often due to insufficient energy delivery in thicker myocardial regions¹⁶. In our study, transmural lesions were only reached in 53% and 5% of the lesions in the equine right and left atrium, respectively. Due to the thicker myocardial wall of horses compared to humans, it can be more difficult to induce transmural lesions and ablate successfully. In human patients, regions with a thicker left atrial wall are associated with sites of electrical reconnection and increased recurrence after pulmonary vein isolation^{16–18}. Thicker tissue is more resistant to ablation due to the need of a deeper lesion to achieve transmural lesions¹⁸. Therefore, the RF delivery needs to be adapted to the local atrial wall thickness by increasing the energy in thicker segments and avoiding high amounts of energy in thinner segments¹⁹. More information is needed in horses about the atrial wall thickness at different locations to titrate RF energy according to the wall thickness. Myocardial sleeves in the caudal vena cava seem to act as a hot spot for arrhythmias in horses and are thus an important target for ablation^{2,20}. This is a thin walled region, so transmural lesions are probably reached more easily compared to the atrial myocardial wall. In this region, RF settings should be lowered to reduce procedure duration and improve safety by avoiding unnecessary RF energy. In thicker segments, RF settings should be increased to improve lesion transmural lesions and thereby lesion durability^{16,17}.

We chose to include the myocardial wall of the right ventricle and not the left ventricle, as the latter has a more trabeculated surface and due to the wall thickness it was more difficult to fit in the *in vitro* set-up. Radiofrequency catheter ablation has not yet been used to treat ventricular arrhythmias in horses. The median right ventricular wall thickness was 16.7 mm and the mean maximum lesion depth, reached with 40 W 60 s, was 5.7 mm. Therefore, ablation of arrhythmias, such as premature depolarizations, that originate from myocardial layers close to the endocardium might be possible, but achieving lesion transmural lesions in the thick ventricular wall seems difficult with the current RF settings. However, there is considerable variation in the right ventricular wall thickness. Depending on the location in the ventricle, it might be feasible to induce transmural lesions at thinner regions. Radiofrequency ablation of ventricular arrhythmias in human medicine are challenging in case of a deep intramural or subepicardial origin, since conventional ablation techniques may be insufficient for inducing transmural lesions^{21–23}. Energy delivery can be impaired when the substrate is ischemic, scar tissue or when it is surrounded by anatomical obstacles, such as epicardial fat or located close to coronary arteries^{23,24}. Therefore, strategies to increase lesion depth, such as RF needle ablation or bipolar ablation, have been developed^{25,26}. Radiofrequency needle ablation, for example, delivers RF energy directly into the myocardium by an extendable/retractable needle, resulting in deep, transmural lesions²⁶. If ventricular arrhythmias are to be treated in horses, these techniques should be further investigated to obtain transmural lesions in the thick myocardial wall.

In addition to the conventional settings, we also included 60 W for 10 s in our experiment. High-power, short-duration ablation is an emerging ablation strategy in human medicine and applies a power of 45–70 W for a short duration of 5–10 s, which might limit catheter instability and tissue oedema^{8,27,28}. This strategy changes

the relationship between resistive and conductive heating, towards predominantly resistive heating. Increasing resistive heating allows immediate heating and permanent tissue injury, while shortening the conductive heating phase limits collateral tissue damage^{8,27,29}. Clinical studies in human medicine showed that high-power, short-duration ablation resulted in decreased recurrence of atrial arrhythmias, lower acute pulmonary vein reconnection, higher rates of first pass isolation and shorter procedure times, with no difference in safety^{29,30}. Animal studies demonstrated that high-power, short-duration ablation lesions were wider and have a similar or lower depth compared to conventional ablation lesions^{8,27,31,32}. In our study, 60 W 10 s resulted in a significantly smaller lesion depth and diameter compared with the other settings. No significant difference was observed in lesion depth and diameter between 60 W 10 s and 30 W 30 s. The effectiveness of high-power, short-duration is questionable in horses, with insufficient lesion depth being a concern when ablating the thicker atrial tissue of horses. Indeed, 60 W 10 s only induced 17% transmural lesions in the right atrium, in contrast to 40 W 60 s which induced 70% transmural lesions. However, this could be a useful strategy when ablating thinner tissue such as the myocardial sleeves of the caudal vena cava, which has a thickness of +/- 1.6 mm²⁰. Pulsed field ablation, a novel energy source, is increasingly used in human medicine. This technique is based on a non-thermal mechanism by which high-voltage electric pulses are used to create pores in the cellular membrane, leading to cellular death^{33,34}. The advantages of pulsed field ablation are the speed of lesion creation and the higher tissue selectivity, which can limit collateral damage and increase procedural safety^{33,35}. This novel ablation approach can be further investigated in the horse to improve safety of ablation at thinner regions and decrease procedure time.

Impedance drop during RF ablation is a specific marker of local tissue heating and is therefore used as a real-time marker of lesion creation in human medicine^{3,36}. As tissue temperature rises during ablation, ion mobility within the heated tissue increases, resulting in a decrease in impedance to current flow^{3,36}. In our study, impedance drop was positively correlated with lesion dimensions: a higher drop led to larger lesion sizes, which corresponds to other studies^{37–39}. The balance between efficacy and safety must be respected. Large impedance drops reflect excessive tissue heating and steam pops³. The operator can alter modifiable factors such as contact force, catheter orientation or power in order to achieve an impedance drop of at least 10 Ω ³⁶.

The depth of the right atrial lesions differed significantly from the depth of left atrial and ventricular lesions. This can be explained by the significantly thinner right atrial wall, which limits lesion depth because lesion transmural is already reached. Indeed, lesion depth in the right atrium was correlated with wall thickness. These tissue differences are therefore related to wall thickness, rather than differences in the tissue itself. Nonetheless, *in vivo* studies have shown that the ablation site can have an effect on lesion dimensions due to differences in local blood flow. For power-controlled ablation, regions with a higher blood flow velocity will have smaller lesions volumes for the same RF settings than sites with low blood flow, due to increased energy loss into the blood pool^{40–42}. On the other hand, due to increased convective cooling, power can be increased without the risk of overheating at the electrode-tissue surface. This allows for more power to be delivered in the tissue and thereby increasing the depth of tissue heating³. In our study, flow velocity was kept constant for the different tissues.

Ex vivo and *in vivo* animal models are commonly used for catheter ablation studies⁴³. Different animal species, such as dogs, cattle, swine and sheep are used in these models, without taking potential species differences in ablation lesion dimensions into account. In our experiment, we compared lesions induced in equine myocardium with those in swine myocardium. Both in the horse heart and in the swine heart, lesion size increased with increasing power or duration. Lesion diameter in equine myocardium was significantly larger than in swine myocardium, although lesion depth and volume did not differ significantly. The impedance was significantly higher in swine ventricular tissue compared to equine ventricular tissue, which could be a possible explanation for the smaller lesion diameter in swine tissue. Indeed, lesion size is determined by the amount of current delivered into the tissue which is inversely proportional to the resistance of the circuit. As such, a higher resistance results in lower current output and smaller lesions. Smaller lesion dimensions at a higher baseline impedance have been described previously⁷. The difference in impedance between horses and swine can be allocated to a difference in intrinsic tissue properties³. Horses have a different extracellular matrix composition (personal data) which might influence impedance. It is known that fibrosis exhibits a lower impedance^{44,45}. The horses in this study were older than the pigs and increasing age results in accumulation of collagen⁴⁶. In addition, athletic horses have more myocardial fibrosis compared to sedentary horses⁴⁷, which could also have played a role. The higher baseline impedance in swine could be an explanation for the higher impedance drop⁴⁸. Lacko et al.⁴³ compared lesion depths in a canine *in vivo* thigh model with a swine *in vitro* model. No significant differences in lesion depth were demonstrated and both models had a similar increasing trend in ablation depth with increased power levels. However, lesion diameters were not studied. The observed difference in diameter in our experiment is relatively small, but demonstrates that the species of the experimental animal used in an *in vitro* model can be of importance. All parameters were kept identical except for species, allowing the effect of species to be examined. However, additional interspecies differences can influence lesion dimensions *in vivo*, such as the size of the heart, heart rate and blood flow.

Using an *in vitro* model has the benefit of standardized RF applications performed under ideal circumstances, which is at the same time also a limitation. Contact force was held constant, so the model does not account for catheter stability, cardiac and respiratory motion, which may influence lesion formation *in vivo*⁶. Tissue perfusion was also not considered in this experiment, which is known to reduce thermal heating of the tissue⁴⁹. The lack of active perfusion could have possibly allowed for ischemic injury⁵⁰. In addition, the time lag between euthanasia or slaughter and execution of the experiments could have induced changes in the viability of the myocardium, possibly influencing lesion formation. However, experiments were started within one hour after euthanasia/slaughter and the different tissue strips and settings were used in a random order. In this study, lesion size was investigated but adverse effects such as collateral injury were not explored. This is especially important

in the thinner right atrium, where lesion transmuralit y was reached in 53% of the RF applications. There were no steam pops observed in this study, but since the tissue used in the in vitro model is not as viable and therefore not as susceptible to tissue boiling, the risk for steam pops does not correspond to the in vivo situation⁶. No antemortem or histopathological examinations were performed to confirm absence of myocardial disease. The findings only apply to the selected ablation settings. The effect of power and duration at higher powers or longer duration are unknown.

Conclusion

Increasing power or duration increased lesion depth, diameter and volume. Power-duration settings should be tailored to the wall thickness that is ablated to optimize lesion formation and induce durable, transmural lesions.

This study showed a significant difference in diameter between equine and swine tissue. Although the difference was relatively small, this means that there are possibly species-related tissue differences that affect RF ablation lesions. Therefore, one should be careful to extrapolate ablation data between species.

Data availability

The datasets generated and/or analysed during the current study are available from the corresponding author on reasonable request.

Received: 2 February 2024; Accepted: 26 September 2024

Published online: 02 October 2024

References

- Buschmann, E. et al. Three-dimensional electro-anatomical mapping and radiofrequency ablation as a novel treatment for atrioventricular accessory pathway in a horse: a case report. *J. Vet. Intern. Med.* **37**, 728–734. <https://doi.org/10.1111/jvim.16668> (2023).
- Van Steenkiste, G. et al. Detection of the origin of atrial tachycardia by 3D electro-anatomical mapping and treatment by radiofrequency catheter ablation in horses. *J. Vet. Intern. Med.* **36**, 1481–1490. <https://doi.org/10.1111/jvim.16473> (2022).
- Issa, Z. M. & Zipes, J. M. *DP In Clinical Arrhythmology and Electrophysiology Ch. Ablation Energy Sources* 206–237 (Elsevier, 2019).
- Kowalski, M. et al. Histopathologic characterization of chronic Radiofrequency ablation lesions for pulmonary vein isolation. *J. Am. Coll. Cardiol.* **59**, 930–938. <https://doi.org/10.1016/j.jacc.2011.09.076> (2012).
- Hindricks, G. ESC Guidelines for the diagnosis and management of atrial fibrillation developed in collaboration with the European Association of Cardio-Thoracic Surgery. *Eur Heart J* **42**, <https://doi.org/10.1093/eurheartj/ehaa798> (2021).
- Borne, R. T. et al. Longer Duration Versus increasing Power during Radiofrequency ablation yields different ablation lesion characteristics. *JACC Clin. Electrophysiol.* **4**, 902–908. <https://doi.org/10.1016/j.jacep.2018.03.020> (2018).
- Bhaskaran, A. et al. Circuit Impedance could be a crucial factor influencing Radiofrequency ablation efficacy and safety: a myocardial Phantom Study of the Problem and its correction. *J. Cardiovasc. Electr.* **27**, 351–357. <https://doi.org/10.1111/jce.12893> (2016).
- Barkagan, M. et al. High-power and short-duration ablation for pulmonary vein isolation: safety, efficacy, and long-term durability. *J. Cardiovasc. Electrophysiol.* **29**, 1287–1296. <https://doi.org/10.1111/jce.13651> (2018).
- Wittkamp, F. H., Hauer, R. N. & de Robles, E. O. Control of radiofrequency lesion size by power regulation. *Circulation.* **80**, 962–968. <https://doi.org/10.1161/01.cir.80.4.962> (1989).
- Nath, S. & Haines, D. E. Biophysics and Pathology of Catheter Energy Delivery systems. *Prog Cardiovasc. Dis.* **37**, 185–204. [https://doi.org/10.1016/S0033-0620\(05\)80006-4](https://doi.org/10.1016/S0033-0620(05)80006-4) (1995).
- Haines, D. E. Determinants of lesion size during radiofrequency catheter ablation: the role of electrode-tissue contact pressure and duration of energy delivery. *J. Cardiovasc. Electrophysiol.* **2**, 509–515 (1991).
- Neuzil, P. et al. Electrical reconnection after pulmonary vein isolation is contingent on Contact Force during initial treatment results from the EFFICAS I study. *Circulation-Arrhythmia Electrophysiol.* **6**, 327–333. <https://doi.org/10.1161/Circep.113.000374> (2013).
- Shah, D. C. et al. Area under the real-time contact force curve (force-Time integral) predicts Radiofrequency Lesion size in an in vitro contractile model. *J. Cardiovasc. Electr.* **21**, 1038–1043. <https://doi.org/10.1111/j.1540-8167.2010.01750.x> (2010).
- Mulder, M. J., Kemme, M. J. B. & Allaart, C. P. Radiofrequency ablation to achieve durable pulmonary vein isolation. *Europace.* **24**, 874–886. <https://doi.org/10.1093/europace/euab279> (2022).
- Buschmann, E. et al. Successful caudal vena cava and pulmonary vein isolation in healthy horses using 3D electro-anatomical mapping and a contact force-guided ablation system. *Equine Vet. J.* <https://doi.org/10.1111/evj.14037> (2023).
- Falascioni, G. et al. Personalized pulmonary vein antrum isolation guided by left atrial wall thickness for persistent atrial fibrillation. *Europace* <https://doi.org/10.1093/europace/euad118> (2023).
- Mulder, M. J. et al. Impact of local left atrial wall thickness on the incidence of acute pulmonary vein reconnection after Ablation Index-guided atrial fibrillation ablation. *Ijc Heart Vasc* **29**, <https://doi.org/10.1016/j.ijcha.2020.100574> (2020).
- Inoue, J., Skanes, A. C., Gula, L. J. & Drangova, M. Effect of Left Atrial Wall Thickness on Radiofrequency ablation success. *J. Cardiovasc. Electr.* **27**, 1298–1303. <https://doi.org/10.1111/jce.13065> (2016).
- Teres, C. et al. Personalized paroxysmal atrial fibrillation ablation by tailoring ablation index to the left atrial wall thickness: the ‘Ablate by-LAW’ single-centre study—a pilot study. *Europace.* **24**, 390–399. <https://doi.org/10.1093/europace/euab216> (2022).
- Ibrahim, L., Buschmann, E., van Loon, G. & Cornillie, P. Morphological evidence of a potential arrhythmogenic substrate in the caudal and cranial vena cava in horses. *Equine Vet. J.* <https://doi.org/10.1111/evj.14075> (2024).
- Sapp, J. L. et al. Deep myocardial ablation lesions can be created with a retractable needle-tipped catheter. *Pacing Clin. Electrophysiol.* **27**, 594–599. <https://doi.org/10.1111/j.1540-8159.2004.00492.x> (2004).
- Berte, B. et al. Irrigated needle ablation creates larger and more transmural ventricular lesions compared with standard unipolar ablation in an ovine model. *Circ. Arrhythm. Electrophysiol.* **8**, 1498–1506. <https://doi.org/10.1161/CIRCEP.115.002963> (2015).
- Futyma, P. et al. Bipolar ablation of refractory atrial and ventricular arrhythmias: importance of temperature values of intracardiac return electrodes. *J. Cardiovasc. Electr.* **30**, 1718–1726. <https://doi.org/10.1111/jce.14025> (2019).
- Futyma, P., Gluszczyk, C. K., Sander, R., Futyma, J. & Kulakowski, M. Bipolar ablation of refractory atrial and ventricular arrhythmias: importance of temperature values of intracardiac return electrodes. *J. Cardiovasc. Electrophysiol.* **30**, 1717–1726 (2019).
- Sandhu, A. & Nguyen, D. T. Forging ahead: update on radiofrequency ablation technology and techniques. *J. Cardiovasc. Electrophysiol.* **31**, 360–369. <https://doi.org/10.1111/jce.14317> (2020).
- Dukkipati, S. R. et al. Intramural Needle Ablation for refractory premature ventricular contractions. *Circ. Arrhythm. Electrophysiol.* **15**, e010020. <https://doi.org/10.1161/CIRCEP.121.010020> (2022).

27. Leshem, E. et al. High-power and short-duration ablation for pulmonary vein isolation: Biophysical characterization. *JACC Clin. Electrophysiol.* **4**, 467–479. <https://doi.org/10.1016/j.jacep.2017.11.018> (2018).
28. Qiu, J., Wang, Y., Wang, D. W., Hu, M. & Chen, G. Update on high-power short-duration ablation for pulmonary vein isolation. *J. Cardiovasc. Electrophysiol.* **31**, 2499–2508. <https://doi.org/10.1111/jce.14649> (2020).
29. Lee, A. C. et al. A Randomized Trial of High vs Standard Power Radiofrequency Ablation for pulmonary vein isolation: SHORT-AF. *JACC Clin. Electrophysiol.* **9**, 1038–1047. <https://doi.org/10.1016/j.jacep.2022.12.020> (2023).
30. Ravi, V. et al. High-power short duration vs. conventional radiofrequency ablation of atrial fibrillation: a systematic review and meta-analysis. *Europace*. **23**, 710–721. <https://doi.org/10.1093/europace/euaa327> (2021).
31. Bhaskaran, A. et al. Five seconds of 50–60 W radio frequency atrial ablations were transmural and safe: an in vitro mechanistic assessment and force-controlled in vivo validation. *Europace*. **19**, 874–880. <https://doi.org/10.1093/europace/euw077> (2017).
32. Bourier, F. et al. High-power short-duration versus standard radiofrequency ablation: insights on lesion metrics. *J. Cardiovasc. Electrophysiol.* **29**, 1570–1575. <https://doi.org/10.1111/jce.13724> (2018).
33. Di Biase, L., Diaz, J. C., Zhang, X. D. & Romero, J. Pulsed field catheter ablation in atrial fibrillation. *Trends Cardiovasc. Med.* **32**, 378–387. <https://doi.org/10.1016/j.tcm.2021.07.006> (2022).
34. Shtembari, J. et al. Efficacy and Safety of Pulsed Field Ablation in Atrial Fibrillation: A Systematic Review. *J. Clin. Med.* **12**, <https://doi.org/10.3390/jcm12020719> (2023).
35. De Asmundis, C. & Chierchia, G. B. Pulsed field ablation: have we finally found the holy grail?. *Europace* **23**, 1691–1692. <https://doi.org/10.1093/europace/euab169> (2021).
36. Chinitz, J. S., Michaud, G. F. & Stephenson, K. Impedance-guided Radiofrequency ablation: using impedance to improve ablation outcomes. *J. Innov. Card Rhythm Manag.* **8**, 2868–2873. <https://doi.org/10.19102/icrm.2017.081003> (2017).
37. Avitall, B., Mughal, K., Hare, J., Helms, R. & Krum, D. The effects of electrode-tissue contact on radiofrequency lesion generation. *Pace*. **20**, 2899–2910. <https://doi.org/10.1111/j.1540-8159.1997.tb05458.x> (1997).
38. Ikeda, A. et al. Relationship between Catheter Contact Force and Radiofrequency Lesion size and incidence of Steam Pop in the beating Canine Heart Electrogram Amplitude, Impedance, and Electrode Temperature are poor predictors of Electrode-Tissue Contact Force and lesion size. *Circulation-Arrhythmia Electrophysiol.* **7**, 1174–1180. <https://doi.org/10.1161/Circep.113.001094> (2014).
39. Chinitz, J. S. et al. Sites with small impedance decrease during catheter ablation for Atrial Fibrillation are Associated with Recovery of Pulmonary Vein Conduction. *J. Cardiovasc. Electrophysiol.* **27**, 1390–1398. <https://doi.org/10.1111/jce.13095> (2016).
40. Tungjatkusolmun, S. et al. Guidelines for predicting lesion size at common endocardial locations during radio-frequency ablation. *Ieee T Bio-Med Eng.* **48**, 194–201. <https://doi.org/10.1109/10.909640> (2001).
41. Petersen, H. H., Chen, X., Pietersen, A., Svendsen, J. H. & Haunso, S. Lesion dimensions during temperature-controlled radiofrequency catheter ablation of left ventricular porcine myocardium - impact of ablation site, electrode size, and convective cooling. *Circulation*. **99**, 319–325. <https://doi.org/10.1161/01.Cir.99.2.319> (1999).
42. Petersen, H. H., Chen, X., Pietersen, A., Svendsen, J. H. & Haunso, S. Lesion size in relation to ablation site during radiofrequency ablation. *Pace*. **21**, 322–326. <https://doi.org/10.1111/j.1540-8159.1998.tb01114.x> (1998).
43. Lacko, C. S. et al. Development of a clinically relevant ex vivo model of cardiac ablation for testing of ablation catheters. *J. Cardiovasc. Electr.* **34**, 682–692. <https://doi.org/10.1111/jce.15768> (2023).
44. Münkler, P. et al. Local impedance guides catheter ablation in patients with ventricular tachycardia. *J. Cardiovasc. Electr.* **31**, 61–69. <https://doi.org/10.1111/jce.14269> (2020).
45. Jacobson, J. T. et al. Tissue-specific variability in human epicardial impedance. *J. Cardiovasc. Electrophysiol.* **22**, 436–439. <https://doi.org/10.1111/j.1540-8167.2010.01929.x> (2011).
46. Lu, L. et al. Cardiac fibrosis in the ageing heart: contributors and mechanisms. *Clin. Exp. Pharmacol. Physiol.* **44**, 55–63. <https://doi.org/10.1111/1440-1681.12753> (2017).
47. Nath, L. C. et al. Histological evaluation of cardiac remodelling in equine athletes. *Sci. Rep.* **14**, 16709. <https://doi.org/10.1038/s41598-024-67621-6> (2024).
48. Qu, L. J. et al. Effect of Baseline Impedance in Radiofrequency Delivery on Lesion Characteristics and the Relationship Between Impedance and Steam Pops. *Front. Cardiovasc. Med.* <https://doi.org/10.3389/fcvm.2022.872961> (2022).
49. Bourier, F. et al. RF electrode-tissue coverage significantly influences steam pop incidence and lesion size. *J. Cardiovasc. Electrophysiol.* **32**, 1594–1599. <https://doi.org/10.1111/jce.15063> (2021).
50. Olson, M. D. et al. Effect of catheter movement and contact during application of radiofrequency energy on ablation lesion characteristics. *J. Interv Card Electr.* **38**, 123–129. <https://doi.org/10.1007/s10840-013-9824-4> (2013).

Acknowledgements

The authors would like to thank the engineering students Arnoud Beyne, Iben Braeckvelt, Dario de Loof, Casper De Somer and Louise vander Heyde, for their help in developing the in vitro model.

Author contributions

EB is the corresponding author. Study design: EB, GVS, MD, PS, GvL, AD. Data collection and study execution: EB, LI, GVS. Data analysis and interpretation: EB, GVS, GvL, AD. Preparation of the manuscript: EB, GVS, MD, PS, LI, GvL, AD.

Declarations

Competing interests

The authors declare no competing interests.

Additional information

Supplementary Information The online version contains supplementary material available at <https://doi.org/10.1038/s41598-024-74486-2>.

Correspondence and requests for materials should be addressed to E.B.

Reprints and permissions information is available at www.nature.com/reprints.

Publisher's note Springer Nature remains neutral with regard to jurisdictional claims in published maps and institutional affiliations.

Open Access This article is licensed under a Creative Commons Attribution-NonCommercial-NoDerivatives 4.0 International License, which permits any non-commercial use, sharing, distribution and reproduction in any medium or format, as long as you give appropriate credit to the original author(s) and the source, provide a link to the Creative Commons licence, and indicate if you modified the licensed material. You do not have permission under this licence to share adapted material derived from this article or parts of it. The images or other third party material in this article are included in the article's Creative Commons licence, unless indicated otherwise in a credit line to the material. If material is not included in the article's Creative Commons licence and your intended use is not permitted by statutory regulation or exceeds the permitted use, you will need to obtain permission directly from the copyright holder. To view a copy of this licence, visit <http://creativecommons.org/licenses/by-nc-nd/4.0/>.

© The Author(s) 2024